International Journal of Chemical Kinetics

WILEY

RESEARCH ARTICLE OPEN ACCESS

Atmospheric Chemistry of $CF_3C(Cl)=CH_2$ (HCFO-1233xf)

Bethanie Curiel[1] | Connor Blair[1] | Morten Frausig[2] | Luisa Pennacchio[2] | Thomas G. Minehan[1] | Ole John Nielsen[2] | Mads P. Sulbaek Andersen[1,2]

[1]Department of Chemistry and Biochemistry, California State Northridge, Northridge, California, USA | [2]Copenhagen Center for Atmospheric Research, Department of Chemistry, University of Copenhagen, Copenhagen, Denmark

Correspondence: Mads P. Sulbaek Andersen (sulbaek.andersen@csun.edu)

Received: 8 January 2026 | **Revised:** 4 May 2026 | **Accepted:** 11 May 2026

ABSTRACT

2-chloro-3,3,3-trifluoropropene, $CF_3C(Cl)=CH_2$ (HCFO-1233xf), is a volatile hydrochlorofluoroolefin, commonly used in industrial synthesis of other halogenated olefins. Kinetics and reaction mechanisms for the reactions of OH radicals, Cl atoms, and O_3 with $CF_3C(Cl)=CH_2$ were investigated using FTIR/smog chamber studies in 700 Torr of air/N_2 diluent at 295 ± 2 K. The rate constants $k(Cl + CF_3C(Cl)=CH_2) = (8.3 \pm 1.1) \times 10^{-11}$, $k(OH + CF_3C(Cl)=CH_2) = (3.4 \pm 0.8) \times 10^{-12}$ and $k(O_3 + CF_3C(Cl)=CH_2) = (2.5 \pm 0.1) \times 10^{-21}$ cm^3 molecule^{-1} s^{-1}, were measured. An atmospheric lifetime of 3.3 days for $CF_3C(Cl)=CH_2$ was determined, dominated by reaction with OH radicals. The reaction of OH radicals and Cl atoms with $CF_3C(Cl)=CH_2$ proceeds by addition to the double bond, and primary and secondary products of the reactions were quantified. Approximately 90% of Cl atoms undergo addition to the terminal carbon. We were unable to establish any preference of reaction site of the OH addition. Reaction of O_3 with $CF_3C(Cl)=CH_2$ leads to the formation of Criegee intermediates that decompose yielding $CF_3C(O)Cl$ and HC(O)H as major products. An upper limit of < 0.3% for the yield CF_3Cl was estimated. The integrated IR absorption cross-section for $CF_3C(Cl)=CH_2$ is (1.22 ± 0.06) × 10^{-16} cm molecule^{-1} (600–1800 cm^{-1}). The effective radiative efficiency was determined as 0.007 W m^{-2} ppb^{-1} leading to a Global Warming Potential (GWP) for the 100-year time horizon of 0.031. The environmental impact of release of $CF_3C(Cl)=CH_2$ to the atmosphere is discussed.

1 | Introduction

The environmental impacts of the emission of chlorofluorocarbons (CFCs), and some of their replacements, into the atmosphere are well documented [1–3]. These compounds were used as refrigerants and propellants and are regulated under the Montreal Protocol and its amendments. The primary objective of the Montreal Protocol was to protect the ozone layer by replacing CFCs with alternative compounds with small environmental impacts. More recently, concern has been raised about some of these replacement compounds due to their impact on global climate. Saturated hydrofluorocarbons (HFCs) do not deplete the ozone due to lack of chlorine in their structure but do contribute to the radiative forcing of climate [4]. Haloolefins are a class of alternatives used to replace HFCs. Due to the high reactivity of the double bond towards OH radicals, the atmospheric lifetime of the olefins are days to weeks and the resulting global warming potentials (GWPs) tend to be small in comparison to the compounds that they are replacements for. HCFO-1233xf (2-chloro-3,3,3-trifluoropropene, $CF_3C(Cl)=CH_2$) is a readily available hydrochlorofluoroolefin. To our knowledge, it is not used as a direct CFC replacement, but is used in the synthesis of other halogenated olefins, including HFO-1234yf ($CF_3CF=CH_2$) [5–8]. HCFO-1233xf contains a chlorine atom that could, in principle, participate in ozone depletion. However, if released to the atmosphere, due to the short lifetime of HCFOs, they will not persist long enough to undergo transportation to the stratosphere. Therefore, directly they will not play a discernable role in stratospheric ozone depletion. This is the first comprehensive study of the atmospheric chemistry of $CF_3C(Cl)=CH_2$.

McGillen et al. [9] reported a rate constant for the reaction of O_3 with $CF_3C(Cl)=CH_2$ and more recently, Garavagno et al. [10] reported the yield of CFC-13 (CF_3Cl) from this reaction. CFC-13 is a long-lived ozone depleting substance with an ozone depletion potential (ODP) of 0.3, an atmospheric lifetime of 640 years and a 100-year GWP of 16300 [11]. The present work improves our understanding of the atmospheric chemistry of HCFO-1233xf specifically, and of halogenated olefins in general. Experiments have been performed using photoreactors at California State University Northridge (CSUN) and Copenhagen Center for Atmospheric Research (CCAR) at University of Copenhagen, Denmark.

2 | Experimental

The photoreactor at CSUN is a 147 L quartz multi-pass cell connected to a Mattson Sirus 100 FTIR spectrometer. The reactor is surrounded by 16 UV-B and 16 UV-C lamps, which were used to initiate the photochemistry. Experiments were conducted in 700 Torr of air or N_2 diluent at 295 ± 2 K. Infrared spectra were obtained from 32 co-added interferograms with 0.25 cm^{-1} spectra resolution and an optical pathlength of 24.44 m. The following absorption features for reactant and references were observed: C_2H_2, 650–800 cm^{-1}; C_2H_4, 650–800 cm^{-1}; C_2H_6, 650–800 cm^{-1}; HCFO-1233xf, 1000–1200 cm^{-1}.

The CCAR photoreactor is a 101 L quartz multi-pass reactor with an optical pathlength of 44.63 m, and interfaced with a Bruker IFS 70v FTIR spectrometer. All experiments were conducted at 296 ± 1 K in 700 Torr of air, with IR spectra recorded as 64 co-added interferograms at a spectral resolution of 0.25 cm^{-1}.

Both at CCAR and at CSUN, a commercial ozone generator (*O_3 Technology*, dielectric barrier discharge; model AC-20) was used to generate O_3, which was then concentrated on cooled silica gel in a trap. This reduces the amount of O_2 introduced to the chamber in the O_3 experiments.

Cl atoms were generated by photolyzing Cl_2 using UV-B lamps

$$Cl_2 + h\nu \rightarrow 2Cl \tag{1}$$

In this work, the study of the chemistry of hydroxyl radicals (OH) utilized two different radical sources: a) UV-B photolysis of methyl nitrite (CH_3ONO) in air in the presence of nitric oxide;

$$CH_3ONO + h\nu \rightarrow CH_3O + NO \tag{2}$$

$$CH_3O + O_2 \rightarrow HO_2 + HC(O)H \tag{3}$$

$$HO_2 + NO \rightarrow OH + NO_2 \tag{4}$$

or b) photolysis of O_3 in the presence of H_2 using UV-C radiation:

$$O_3 + h\nu \rightarrow O(^1D) + O_2 \tag{5}$$

$$H_2 + O(^1D) \rightarrow OH + H \tag{6}$$

$$O_3 + H \rightarrow OH + O_2 \tag{7}$$

Reference spectra were recorded for this work by expanding known volumes of the compounds into the chambers. Analysis of product and reactant concentrations in the recorded spectra was achieved through a process of "spectral stripping" in which fractions of the reference spectrum were incrementally subtracted from the sample spectrum. The relative rate method is a well-known technique widely employed in the study of the kinetics of reactions of Cl atom and OH radical reactions with hydrocarbons. Plotting the logarithmic decay of the reference and reactants the following expression allows determination of the unknown rate constants:

$$\ln\left(\frac{[\text{HCFO-1233xf}]_{t_0}}{[\text{HCFO-1233xf}]_t}\right) = \frac{k_{\text{HCFO-1233xf}}}{k_{\text{Reference}}} \times \ln\left(\frac{[\text{Reference}]_{t_0}}{[\text{Reference}]_t}\right) \tag{I}$$

In Equation (I), $k_{\text{HCFO-1233xf}}$ and $k_{\text{Reference}}$ are the rate constants for the reactions of Cl atoms or OH radicals with the HCFO and the reference compound, respectively and the terms $[\text{HCFO-1233xf}]_t$, $[\text{HCFO-1233xf}]_{t_0}$, $[\text{Reference}]_t$, and $[\text{Reference}]_{t_0}$, denote the concentrations of the reactant and reference at time t_0 (initial) and time t. A linear least squares fit to the data gives a slope which is the ratio of the rate constants for the reaction of Cl atoms or OH radicals with HCFO-1233xf and reference compound. All uncertainties stated are two standard deviations from least square regressions analysis, forced through zero, and includes a ± 5% estimated error for the IR spectrum analysis of reactant and reference.

The O_3 kinetics were determined using the absolute rate method, by observing the pseudo first order loss of the reactant under conditions of excess ozone. Plotting the pseudo-first order rate constants obtained versus the initial ozone concentrations produces a linear relationship with slope of k_8

$$O_3 + CF_3C(Cl)=CH_2 \rightarrow \text{Products} \tag{8}$$

Cyclohexane, *c*-C_6H_{12}, was added to the reaction mixtures as an OH scavenger to avoid any potential interference with the measured loss of $CF_3C(Cl)=CH_2$. Control experiments were performed to determine unwanted loss of reactants, reference compounds or products via photolysis, heterogeneous reactions or chemistry occurring in the dark. Mixtures of HCFO-1233xf and reference compounds were irradiated for 30 min with no measurable change in concentrations, and we conclude that photolytic loss of the reactant and reference compounds are not a complication in the present work. The possibility of heterogeneous reactions was tested by letting reactant/product mixtures stand in the dark in the chamber for 30 min, after UV irradiation had completed. We were unable to identify any observable loss (< 2%) of reactants or products. We conclude that heterogeneous reactions are unlikely to play a role in the present investigations.

HCFO-1233xf was supplied by Matrix Scientific at a 98% purity and underwent repeated freeze-pump-thaw cycles. All other reagents were obtained at high purities (>99%) from commercial vendors.

3 | Results and Discussion

3.1 | Relative Rate Studies of Cl + HCFO-1233xf

The rate constant of reaction (9) was measured relative to the ones of reactions (10), (11) and (12).

$$Cl + CF_3C(Cl)=CH_2 \rightarrow \text{Products} \quad (9)$$

$$Cl + C_2H_2 \rightarrow \text{Products} \quad (10)$$

$$Cl + C_2H_6 \rightarrow \text{Products} \quad (11)$$

$$Cl + C_2H_4 \rightarrow \text{Products} \quad (12)$$

Mixtures of 5.1–5.7 mTorr of $CF_3C(Cl)=CH_2$, 45–80 mTorr of Cl_2 and either 7.5 mTorr of C_2H_6, 7.8 mTorr of C_2H_4 or 4.7 mTorr of C_2H_2 in a total pressure of 700 Torr of air or N_2. The loss of $CF_3C(Cl)=CH_2$ is plotted as a function of loss of the reference compounds in Figure 1.

A linear least square fit of the data in Figure 1 yields k_9/k_{10} = (1.67 ± 0.04), k_9/k_{11} = (1.39 ± 0.02), and k_9/k_{12} = (0.88 ± 0.01). Using $k_{10} = (5.07 \pm 0.34) \times 10^{-11}$ [12], $k_{11} = (5.7 \pm 0.4) \times 10^{-11}$ [13], and $k_{12} = (9.29 \pm 0.5) \times 10^{-11}$ cm^3 molecule^{-1} s^{-1} [3] gives k_9 = (8.6 ± 0.6), (8.09 ± 0.58) and (8.1 ± 0.4) × 10^{-11} cm^3 molecule^{-1} s^{-1}, respectively. We obtain a final value for k_9 which is the average of the individual determinations reported with error limits that include the extremes of the individual determinations, hence $k_9 = (8.3 \pm 1.1) \times 10^{-11}$ cm^3 molecule^{-1} s^{-1}.

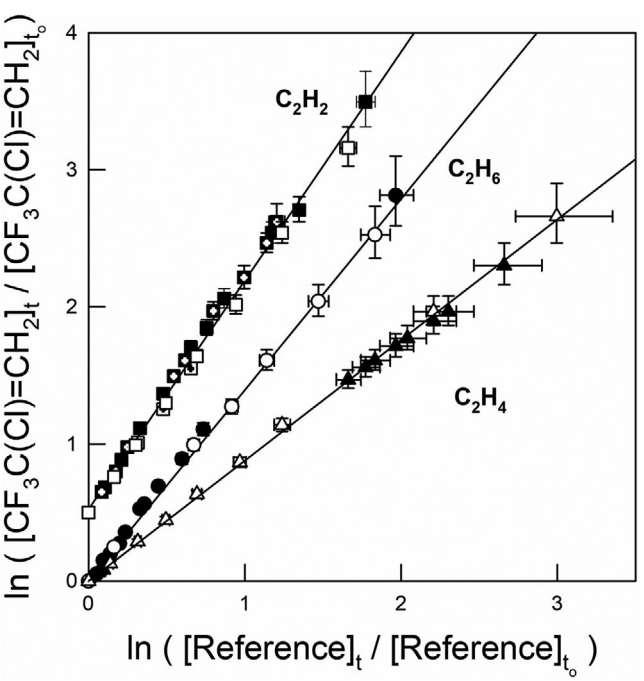

FIGURE 1 | Loss of $CF_3C(Cl)=CH_2$ relative to C_2H_4 (triangles), C_2H_6 (circles) and C_2H_2 (squares). Open and solid symbols indicate data obtained in 700 Torr of N_2 or air, respectively. Experiments conducted at CCAR are represented by cross hair symbols; the rest of the data was obtained at CSUN. C_2H_2 has a 0.5 vertical offset to improve visual clarity and allow for comparison. Error bars reflect the estimated measurement uncertainty.

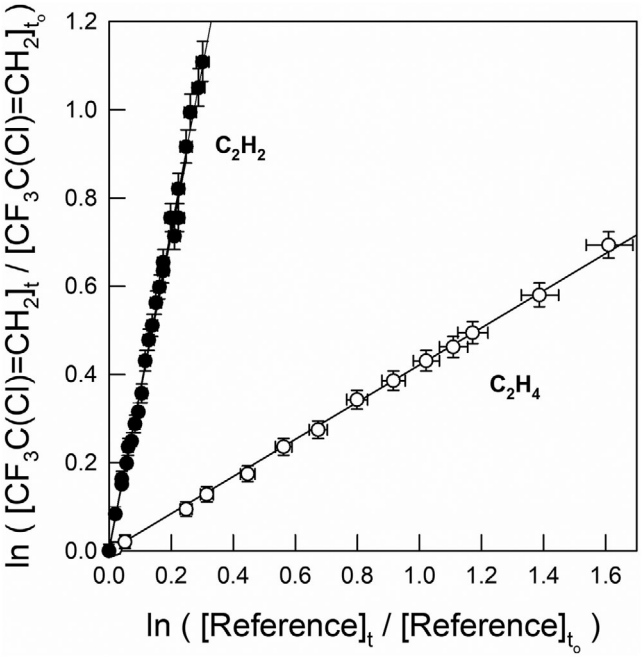

FIGURE 2 | Loss of $CF_3C(Cl)=CH_2$ relative to C_2H_4 (open) and C_2H_2 (solid) in presence of OH radicals in 700 Torr total pressure of air, (295 ± 2) K. C_2H_4 experiment were conducted with added 2.1 mTorr of NO. Error bars reflect the estimated measurement uncertainty.

A literature search revealed no previous studies of the Cl atom kinetics for $CF_3C(Cl)=CH_2$. The two conformers of the structural isomer of $CF_3C(Cl)=CH_2$, (*Z*)-$CF_3CH=CHCl$ and (*E*)-$CF_3CH=CHCl$, have previously been studied, and Cl atom rate constants of $(6.26 \pm 0.84) \times 10^{-11}$ [14] and $(5.22 \pm 0.72) \times 10^{-11}$ cm^3 molecule^{-1} s^{-1} [15], respectively, have been reported. Those values are similar but lower than k_9 determined herein.

3.2 | Relative Rate Study of $CF_3C(Cl)=CH_2$ + OH

The rate of reaction of (13) was measured relative to reference reactions (14) and (15):

$$OH + CF_3C(Cl)=CH_2 \rightarrow \text{Products} \quad (13)$$

$$OH + C_2H_2 \rightarrow \text{Products} \quad (14)$$

$$OH + C_2H_4 \rightarrow \text{Products} \quad (15)$$

Mixtures of 5.1–5.7 mTorr of $CF_3C(Cl)=CH_2$, 92–105 mTorr of CH_3ONO, 0–30 mTorr of NO and either 1.6–3.6 mTorr of C_2H_2 or 7.9 mTorr of C_2H_4 at a total pressure of 700 Torr of air. Figure 2 shows the loss of $CF_3C(Cl)=CH_2$ versus the loss of the two reference compounds. A linear least square fit to the data shown in Figure 2 yields k_{13}/k_{14} = (3.64 ± 0.05), k_{13}/k_{15} = (0.42 ± 0.01). Using $k_{14} = (8.45 \pm 0.85) \times 10^{-12}$ cm^3 molecule^{-1} s^{-1} [16] and $k_{15} = (8.52 \pm 1.28) \times 10^{-12}$ cm^3 molecule^{-1} s^{-1} [17] gives k_{13} = (3.1 ± 0.4) × 10^{-12} and (3.57 ± 0.59) × 10^{-12} cm^3 molecule^{-1} s^{-1},

respectively. We obtain a final value for k_{13} which is the average of the individual determinations reported with error limits, that include the extremes of the individual determinations, hence $k_{13} = (3.4 \pm 0.8) \times 10^{-12}$ cm^3 molecule^{-1} s^{-1}. There are no previous studies of k_{13} in the literature. In the model exercise presented in Garavagno et al. [10], they use a value of 1.31×10^{-12} cm^3 molecule^{-1} s^{-1} for k_{13}, with a reference to Michelat et al. [18]. It is unclear how the value reported for k_{13} in Garavagno et al. was calculated, but it is substantially smaller (factor of 2.5) than the one determined in the present work. As discussed for the Cl atom rate constants in the previous section, the rate constants k(OH + (*Z*)-$CF_3CH{=}CHCl$) and k(OH + (*E*)-$CF_3CH{=}CHCl$) have also been evaluated by IUPAC as 9.24×10^{-13} and 3.53×10^{-13} cm^3 molecule^{-1} s^{-1} [19], respectively. As was the case with the Cl atom reactivity, $CF_3C(Cl){=}CH_2$ reacts faster with OH than its structural conformers (*Z*)-$CF_3CH{=}CHCl$ and (*E*)-$CF_3CH{=}CHCl$ (in this case by a factor of approximately 4).

3.3 | Absolute Rate Study of $CF_3C(Cl){=}CH_2 + O_3$

The rate constant for the reaction of $CF_3C(Cl){=}CH_2$ with O_3 (k_8) was investigated by observing the loss of the compound in the presence of excess O_3. Mixtures of 5.1–5.7 mTorr of $CF_3C(Cl){=}CH_2$, and 0.35–2.8 mTorr O_3 in air at 700 Torr total pressure. An OH radical scavenger, *c*-C_6H_{12} (10–20 mTorr), was added to the reaction mixtures to prevent any OH radicals from reacting with $CF_3C(Cl){=}CH_2$. The loss of $CF_3C(Cl){=}CH_2$ was observed following pseudo first-order kinetics. The pseudo first order decay of $CF_3C(Cl){=}CH_2$ is plotted versus the O_3 concentrations in Figure 3, and a least-squares fit to the data gives a slope of $k_8 = (2.50 \pm 0.10) \times 10^{-21}$ cm^3 molecule^{-1} s^{-1}. In the absence of a scavenger, the observed rate of decay of $CF_3C(Cl){=}CH_2$ was highly elevated (see gray triangles in Figure 3).

McGillen et al. [9] reported a value for k_8 at 298K of $(2.50 \pm 0.36) \times 10^{-21}$ cm^3 molecule^{-1} s^{-1}. The result of the present work and that of McGillen et al. for k_8 are in excellent agreement. For the structural conformers (*E*)-$CF_3CH{=}CHCl$ and (*Z*)-$CF_3CH{=}CHCl$, O_3 rate constant values of (1.46 ± 0.12) [15] and $(1.53 \pm 0.12) \times 10^{-21}$ cm^3 molecule^{-1} s^{-1} [14] have been reported. The reactivities of both these conformers toward O_3 are similar to that of $CF_3C(Cl){=}CH_2$.

3.4 | Infrared Spectrum of $CF_3C(Cl){=}CH_2$

IR spectra were recorded of known concentrations of $CF_3C(Cl){=}CH_2$ introduced into the photochemical reactor at CSUN. Figure 4 shows the IR spectrum of $CF_3C(Cl){=}CH_2$ in 700 Torr of air at 295 ± 2 K. As shown in the insert in Figure 4, the absorption intensity (shown here as the total integrated absorbance) exhibited a linear relationship with increasing $CF_3C(Cl){=}CH_2$ concentrations. The integrated IR absorption cross sections for the individual IR bands are listed in Table 1. Nine distinct absorption bands are readily identifiable in the spectrum. The quoted uncertainty in the infrared spectrum is the propagation of the following contributions: sample concentration (± 2%), path length (± 1.5%), residual baseline offset after subtraction of the background (± 0.5%), and

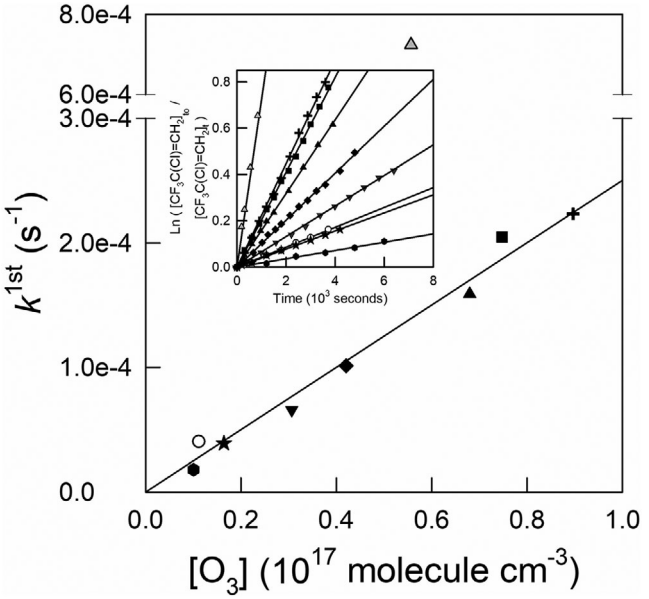

FIGURE 3 | Pseudo-first order loss of $CF_3C(Cl){=}CH_2$ versus various O_3 concentrations in 700 Torr of air diluent at 295 ± 2 K. The inset shows the pseudo first-order kinetics observed. The open circles indicate data collected at CCAR, whereas solid symbols indicate data from experiments conducted at CSUN. The data shown with gray upward triangles were obtained from experiments with no added cyclohexane, but approximately the same concentration of O_3 as in the experiments indicated with the solid upward triangles.

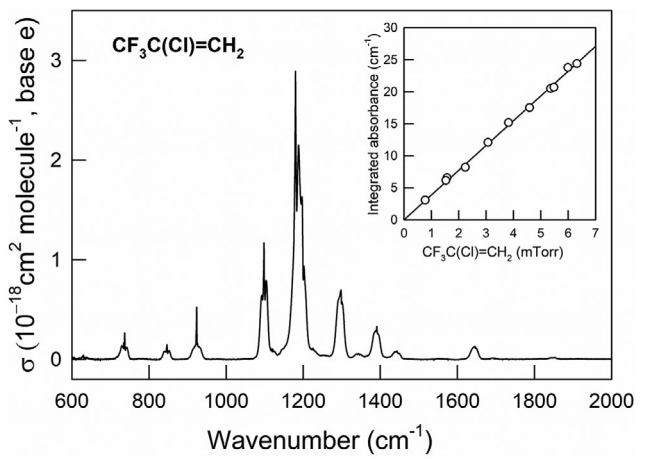

FIGURE 4 | The IR spectrum of $CF_3C(Cl){=}CH_2$ recorded in 700 Torr of air diluent at 295 ± 2 K. Insert shows the calibration based on the integrated absorbance of eight IR bands (see main text for details).

spectrometer accuracy (± 1%). The IR spectrum is also included in table format as Supplemental Information.

3.5 | Product Study of $CF_3C(Cl){=}CH_2 + Cl$

The Cl atom-initiated oxidation mechanism of $CF_3C(Cl){=}CH_2$ was studied using mixtures of 5.0–6.0 mTorr of $CF_3C(Cl){=}CH_2$ and 40.0–70.0 mTorr Cl_2 in 700 Torr air diluent. The mixtures were exposed to 15–360 s total of UV irradiation. $CF_3C(Cl){=}CH_2$ was consumed completely in around 13 s. Continued irradiation

TABLE 1 | Integrated IR cross sections (base e) for $CF_3C(Cl)=CH_2$ determined in the present work (295 ± 2 K, 700 Torr total pressure).

Wavenumber ranges (cm^{-1})	Integrated cross sections ($cm\ molecule^{-1}$)
500–1800	$(1.22 \pm 0.06) \times 10^{-16}$
715–760	$(3.15 \pm 0.16) \times 10^{-18}$
830–860	$(1.85 \pm 0.09) \times 10^{-18}$
900–954	$(4.25 \pm 0.21) \times 10^{-18}$
1070–1130	$(1.78 \pm 0.09) \times 10^{-17}$
1139–1240	$(6.41 \pm 0.32) \times 10^{-17}$
1270–1320	$(1.49 \pm 0.07) \times 10^{-17}$
1328–1464	$(1.02 \pm 0.05) \times 10^{-17}$
1625–1665	$(2.63 \pm 0.13) \times 10^{-18}$

of the mixture revealed the formation of secondary oxidation products.

Figure 5 shows the spectra acquired before (Panel A) and after (Panel B) 6 s of UV-B irradiation. The consumption of $CF_3C(Cl)=CH_2$ was 54%. Subtraction of excess $CF_3C(Cl)=CH_2$ from Panel (B) results in the spectrum shown in Panel (C). Comparison with reference spectra of HC(O)Cl (Panel D), HC(O)H (Panel E) and $CF_3C(O)Cl$ (Panel F) with the product spectrum in Panel (C) show the formation of these three products. The residual spectrum after subtracting excess $CF_3C(Cl)=CH_2$, as well as the three products, is shown in Panel (G). The residual IR features shown in Panel G scaled linearly with one another across spectra collected after different irradiation times. As discussed further below, we assign the spectrum shown in Panel (G) to $CF_3C(O)CH_2Cl$.

Reaction of chlorine atoms with $CF_3C(Cl)=CH_2$ will proceed as addition to either side of the double bond, followed by addition of O_2:

$$Cl + CF_3C(Cl)=CH_2 \rightarrow CF_3ClC(\cdot)–CClH_2 \quad (16a)$$

$$Cl + CF_3C(Cl)=CH_2 \rightarrow CF_3ClCCl–C(\cdot)H_2 \quad (16b)$$

$$CF_3ClC(\cdot)–CClH_2 + O_2 \rightarrow CF_3ClCO_2(\cdot)–CClH_2 \quad (17a)$$

$$CF_3ClCCl–C(\cdot)H_2 + O_2 \rightarrow CF_3ClCCl–CH_2O_2(\cdot) \quad (17a)$$

In the photoreactor, the peroxy radicals formed above react with other peroxy radicals and/or itself. In the atmosphere, $CF_3ClC(O_2)CClH_2$ and $CF_3ClCClCH_2O_2$ are more likely to react with NO and other RO_2 radicals. In both cases the main outcome is the formation of alkoxy radicals:

$$CF_3ClCO_2(\cdot)–CClH_2 + RO_2(\cdot) \rightarrow CF_3ClCO(\cdot)–CClH_2 + RO(\cdot) + O_2 \quad (18a)$$

$$CF_3ClCCl–CH_2O_2(\cdot) + RO_2(\cdot) \rightarrow CF_3ClCCl–CH_2O(\cdot) + RO(\cdot) + O_2 \quad (18b)$$

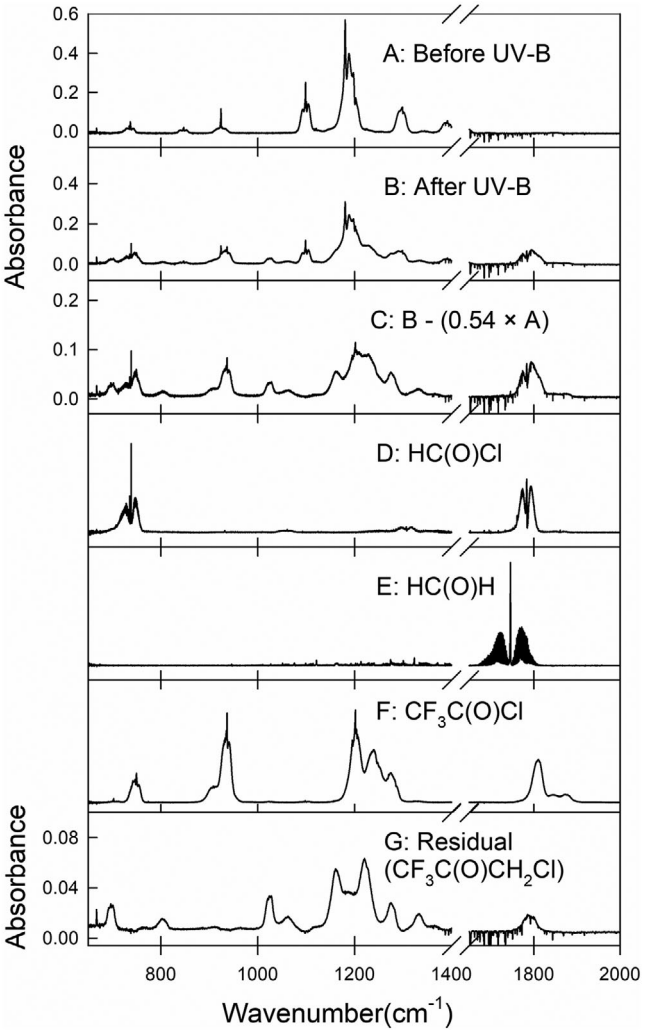

FIGURE 5 | IR spectra observed before (A) and after (B) 6 s of UV-B irradiation of 5.50 mTorr of $CF_3C(Cl)=CH_2$ with 65.85 mTorr of Cl_2 in 700 Torr of air. The consumption of $CF_3C(Cl)=CH_2$ was 54% Panel C shows the residual spectrum after the remaining features of $CF_3C(Cl)=CH_2$ were subtracted. Panels D, E and F are reference spectra of HC(O)Cl, HC(O)H and $CF_3C(O)Cl$, respectively. Panel G shows the residual spectrum (assigned to $CF_3C(O)CH_2Cl$, see text for details) after subtraction of HC(O)Cl, HC(O)H and $CF_3C(O)Cl$ from Panel C.

The resulting alkoxy radicals can undergo decomposition through C–C scission:

$$CF_3ClCO(\cdot)–CClH_2 \rightarrow CF_3C(O)Cl + (\cdot)CH_2Cl \quad (19a)$$

$$CF_3ClCCl–CH_2O(\cdot) \rightarrow HC(O)H + CF_3ClC(\cdot)Cl \quad (19b)$$

or elimination of Cl:

$$CF_3ClCO(\cdot)–CClH_2 \rightarrow CF_3C(O)CH_2Cl + Cl \quad (20)$$

or reaction with O_2:

$$CF_3ClCCl–CH_2O(\cdot) + O_2 \rightarrow CF_3CCl_2CHO + HO_2 \quad (21)$$

The CH_2Cl radical generated in reaction (19a) will react with O_2 and RO_2 to yield HC(O)Cl:

$$(\cdot)CH_2Cl + O_2 \rightarrow (\cdot)O_2CH_2Cl \quad (22)$$

$$(\cdot)O_2CH_2Cl + RO_2 \rightarrow (\cdot)OCH_2Cl + RO(\cdot) + O_2 \quad (23)$$

$$(\cdot)OCH_2Cl + O_2 \rightarrow HC(O)Cl + HO_2 \quad (24)$$

$(\cdot)OCH_2Cl$ can also undergo decomposition to give HCl and HCO, however at one atmosphere of pressure of air, reaction (25) is of minor importance.

$$(\cdot)OCH_2Cl \rightarrow HCl + HCO \quad (25)$$

If $CF_3ClC(\cdot)Cl$ is formed (via reaction 19b), it would likely react with O_2 followed by reaction with other RO_2 radicals to give CF_3CCl_2O radicals. Alkoxy radicals with multiple chlorine substituents in the alpha position undergo predominantly Cl elimination [20]. As such, any $CF_3ClC(\cdot)Cl$ formed in reaction (19b) will end up as $CF_3C(O)Cl$:

$$CF_3ClC(\cdot)Cl + O_2 \rightarrow CF_3CCl_2O_2 \quad (26)$$

$$CF_3CCl_2O_2 + RO_2(\cdot) \rightarrow CF_3CCl_2O + RO(\cdot) + O_2 \quad (27)$$

$$CF_3CCl_2O \rightarrow CF_3C(O)Cl + Cl \quad (28)$$

Based on the considerations above, HC(O)H can only be formed as a primary product in reaction 19b, while HC(O)Cl primarily is a product of reaction (24). $CF_3C(O)Cl$ can be formed both in reaction (19a) and though reactions (19b) followed by (26–28). $CF_3C(O)CH_2Cl$ and CF_3CCl_2CHO, formed in reactions (20) and (21), respectively, are both carbonyl products that are expected to be moderately reactive toward Cl atoms and could also undergo some photolysis under UV-B irradiation.

Figure 6A shows a plot of the formation of HC(O)H, HC(O)Cl and $CF_3C(O)Cl$ and the product with an absorption shown in Figure 5G, normalized to the initial concentration of $CF_3C(Cl)=CH_2$, versus the fractional loss of $CF_3C(Cl)=CH_2$. After $CF_3C(Cl)=CH_2$ had been completely consumed, additional irradiation of up to 6 min total resulted in complete disappearance of the features shown in Figure 5G. As shown in Figure 6B, concurrent consumption of HC(O)Cl (complete) and formation of CF_3OH, COF_2, $CF_3O_3CF_3$ and $CF_3O_2CF_3$ were observed. $CF_3C(O)Cl$ is unreactive in our system, and no additional formation $CF_3C(O)Cl$ was observed from the decay of the product shown in Figure 5G. This latter observation indicated that the main primary degradation product shown in Figure 5G is $CF_3C(O)CH_2Cl$. Reaction of Cl atoms with CF_3CCl_2CHO, would result in CF_3CCl_2O alkoxy radicals that would either decompose to give $COCl_2$ or eliminate a Cl atom to give $CF_3C(O)Cl$. As mentioned above, no additional formation of $CF_3C(O)Cl$ was observed. Using a reference spectrum for $COCl_2$, features due to the formation of this product were also sought in the product spectra for the additional irradiation times, but not observed. On the contrary $CF_3C(O)CH_2Cl$ is expected to give rise to the observed products.

$$CF_3C(O)CH_2Cl + Cl \rightarrow CF_3C(O)CH(\cdot)Cl + HCl \quad (29)$$

$$CF_3C(O)CH(\cdot)Cl + O_2 \rightarrow CF_3C(O)CHClO_2(\cdot) \quad (30)$$

$$CF_3C(O)CHClO_2(\cdot) + RO_2(\cdot) \rightarrow CF_3C(O)CHClO(\cdot) + RO(\cdot) + O_2 \quad (31)$$

$$CF_3C(O)CHClO(\cdot) \rightarrow CF_3C(O)(\cdot) + HC(O)Cl \quad (32)$$

$$CF_3C(O)(\cdot) \rightarrow CF_3(\cdot) + CO \quad (33)$$

$$CF_3C(O)(\cdot) + O_2 \rightarrow CF_3C(O)O_2(\cdot) \quad (34)$$

$$CF_3C(O)O_2(\cdot) + RO_2(\cdot) \rightarrow CF_3C(O)O(\cdot) + RO(\cdot) + O_2 \quad (35)$$

$$CF_3C(O)O(\cdot) \rightarrow CO_2 + CF_3 \quad (36)$$

$$CF_3 + O_2 + M \rightarrow CF_3O_2 + M \quad (37)$$

$$CF_3O_2 + CF_3O_2 + M \rightarrow 2CF_3O + O_2 + M \quad (38)$$

$$CF_3O_2 + CF_3O + M \rightarrow CF_3O_3CF_3 \quad (39)$$

$$CF_3O + CF_3O + M \rightarrow CF_3O_2CF_3 \quad (40)$$

$$CF_3O + R_H \rightarrow CF_3OH + R \quad (41)$$

In reaction (41) R_H represents any species present in the chamber containing hydrogen substituents. The perfluoromethanol, CF_3OH, formed in reaction (41) will undergo thermal decomposition and give COF_2 on a timescale similar to the duration of the experiments:

$$CF_3OH \rightarrow COF_2 + HF \quad (42)$$

HC(O)Cl formed in reaction (24) does not show up in the spectra obtained at the extended irradiation times (see Figure 6B). The reaction of Cl atoms towards HC(O)Cl is fast and likely several orders of magnitude faster than the reaction of Cl with $CF_3C(O)CH_2Cl$ [21], which can explain why we do not observe it as a secondary product. The combined yields of CF_3OH, COF_2, $CF_3O_3CF_3$ and $CF_3O_2CF_3$ result in a straight line (see datapoints marked as stars in Figure 6B) and we use a linear least squares fit to these datapoint to calibrate the spectrum of $CF_3C(O)CH_2Cl$ shown in Figure 5G. Using this approach, we are able to assign absolute values (mTorr) to the *x*-axis in Figure 6B and use this calibration to establish the yield of $CF_3C(O)CH_2Cl$ in the linear least squares analysis in Panel A (56 ± 4) %. Linear least squares fit to the $CF_3C(O)Cl$ data in Figure 6 gives a molar yield of (42 ± 3) %. HC(O)Cl and HC(O)H are formed as primary products but are highly reactive towards Cl atoms themselves:

$$HC(O)Cl + Cl \rightarrow HCl + Products \quad (43)$$

$$HC(O)H + Cl \rightarrow HCl + Products \quad (44)$$

The yields of HC(O)H and HC(O)Cl in Figure 6A can be fitted using expression (II), which is an analytical solution to the kinetic system describing the observed yield of a reactive product in the

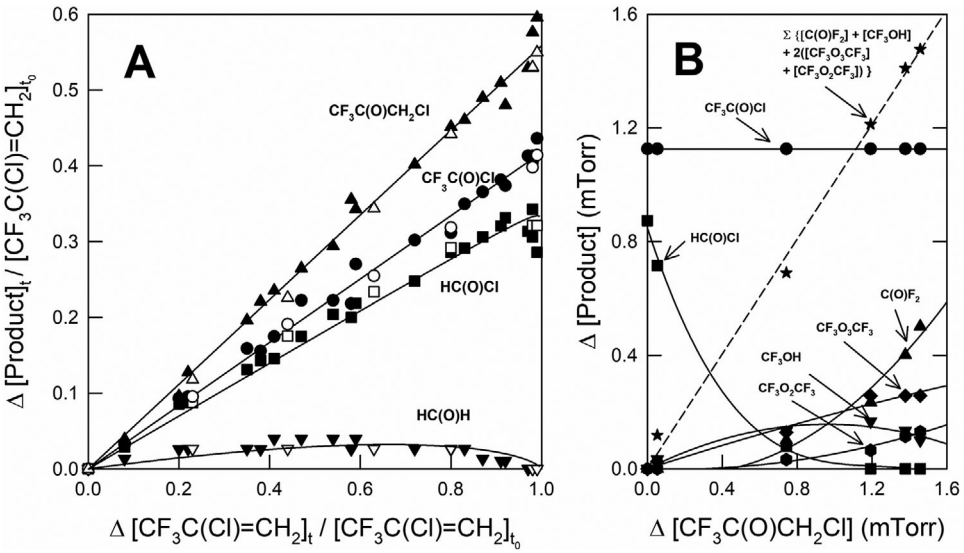

FIGURE 6 | Panel A: Yields of $CF_3C(O)Cl$ (circles), HC(O)Cl (squares) and HC(O)H (downward triangles) and an unknown product with a broad absorbance band at 1791 cm^{-1}(upward triangles), subsequently assigned $CF_3C(O)CH_2Cl$, against the loss of $CF_3C(Cl)=CH_2$, normalized to initial concentration of $CF_3C(Cl)=CH_2$, during the Cl initiated oxidation of $CF_3C(Cl)=CH_2$ in 700 Torr air of diluent. Solid symbols were obtained in 700 Torr of air, while open symbols were obtained in 700 Torr of pure O_2. Fit lines are linear least square regressions or polynomial fits for HC(O)Cl and HC(O)H (see text for details). Panel B: Product yields due to consumption of $CF_3C(O)CH_2Cl$ for extended periods of radiation time, after all $CF_3C(Cl)=CH_2$ has been consumed. Fit lines are either second or third order polynomial fits to aid the eye in interpreting the data, or linear least squares regressions for $CF_3C(O)Cl$ and the datapoints representing the sum of $C(O)F_2$, CF_3OH, $CF_3O_3CF_3$ and $CF_3O_2CF_3$.

chamber [22]:

$$\frac{[\text{HC(O)H or HC(O)Cl}]}{[CF_3C(O)CH_2Cl]_0} = \frac{\alpha}{1-\frac{k_{(4344\ or\ )}}{k_9}}(1-x)\left[(1-x)^{((k_{(4344\ or\ )}/k_9)-1)}-1\right] \quad \text{(II)}$$

where $x = 1 - [CF_3C(O)CH_2Cl]_t / [CF_3C(O)CH_2Cl]_0$ is the fractional consumption of $CF_3C(O)CH_2Cl$ and α is the initial yield of the products from $CF_3C(O)CH_2Cl$ ($0 < \alpha < 1$). Using $k_{43} = 7.76 \times 10^{-13}$ [10], $k_{44} = 7.0 \times 10^{-11}$ [10] and $k_9 = (8.3 \pm 1.1) \times 10^{-11}$ cm^3 $molecule^{-1}$ s^{-1} (this work) give initial yields of HC(O)Cl and HC(O)H of (35 ± 3) % and (8 ± 2) % at 700 and 100 Torr of air, respectively. Both HC(O)Cl and in particular HC(O)H will likely also undergo some photolysis during the experiments, and this is evident from the less than ideal fits to the data (as shown in Figure 6A). Based on the discussion above, it is clear that addition of Cl atoms preferentially occurs at the terminal carbon site (~ 90%), giving rise to the formation of $CF_3C(O)CH_2Cl$ as a major primary product (~55%) and ~35% $CF_3C(O)Cl$ and 35% HC(O)Cl. Approximately 10% of the chlorine addition occurs at the central carbon, giving rise to ~10% yield of both HC(O)H and $CF_3C(O)Cl$.

3.6 | Product Study of $CF_3C(Cl)=CH_2$ + OH

The mechanism of the OH radical initiated oxidation of $CF_3C(Cl)=CH_2$ was investigated using either CH_3ONO or O_3/H_2 as an OH source. Experiments involved irradiation of reaction mixtures of 5.0–6.0 mTorr of $CF_3C(Cl)=CH_2$ 150–200 mTorr of hydrogen and 1–2 Torr of ozone in 700 Torr of air diluent, or 5.6 mTorr $CF_3C(Cl)=CH_2$ and 85.3 mTorr CH_3ONO in 700 Torr of air. Examples of IR spectra recorded are shown in Figure 7: Panel A shows the reaction mixture before irradiation of a mixture consisting of 5.25 mTorr of $CF_3C(Cl)=CH_2$, 169.1 mTorr of hydrogen, and 1–2 Torr of O_3 in 700 Torr of air. After 30 sec of UV-C radiation the consumption of $CF_3C(Cl)=CH_2$ was 50%, and the product spectrum shown in Panel B was obtained. Panel C shows the residual spectrum obtained by subtracting the remaining $CF_3C(Cl)=CH_2$ from Panel B. Comparison of Panel C with reference spectra of $CF_3C(O)Cl$ (panel D) and HC(O)H (panel E) show the formation of these two products. No other products were observed in the reaction.

The product formation as a function of the loss of $CF_3C(Cl)=CH_2$, normalized to the initial concentration of $CF_3C(Cl)=CH_2$, is shown in Figure 8. There were no observable differences in the observed formation of $CF_3C(O)Cl$ using the two OH sources. Note that HC(O)H can only be quantified as an oxidation product for $CF_3C(Cl)=CH_2$ in the experiments using O_3/H_2 as an OH source, as photolysis of CH_3ONO is a significant source of HC(O)H, which would interfere with the product analysis.

A linear least squares fit to the data shown for $CF_3C(O)Cl$ in Figure 8 gives a yield of (95 ± 6) %. The oxidation product HC(O)H also reacts with OH radicals ($k_{(OH+HC(O)H)} = 8.8 \times 10^{-12}$ cm^3 $molecule^{-1}$ s^{-1} [10]) and the product data for HC(O)H was fitted using an equation similar to expression (II), substituting $k_{(OH+HC(O)H)}$ in place for $k_{(44)}$, and $k_{13} = (3.4 \pm 0.8) \times 10^{-12}$ cm^3 $molecule^{-1}$ s^{-1} (this work) in place for k_9, yielding an initial yield of HC(O)H (α in expression II) of (102 ± 6) %.

OH radicals can add to both sides of the double bond in $CF_3C(Cl)=CH_2$:

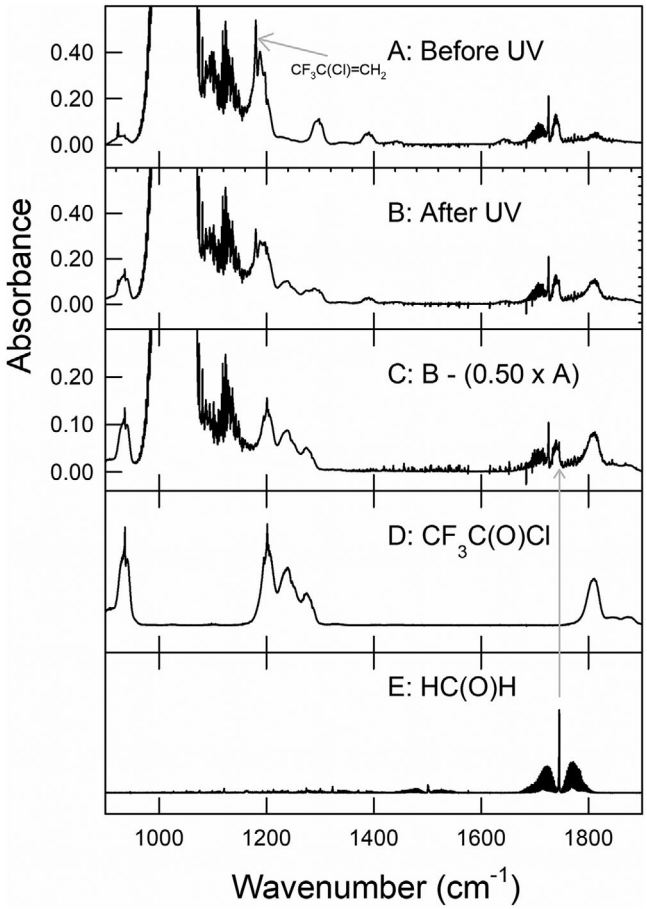

FIGURE 7 | IR spectra obtained before (A) and after (B) 30 s of UV-C irradiation of mixture consisting of 5.25 mTorr of $CF_3(Cl)C{=}CH_2$, 169.1 mTorr of hydrogen, and 2 Torr of O_3 in 700 Torr of air. The consumption of $CF_3(Cl)C{=}CH_2$ was 50%. Panel C shows the products remaining after subtracting features of $CF_3C(Cl){=}CH$. Panels D and E are reference spectra of $CF_3C(O)Cl$ and HC(O)H respectively.

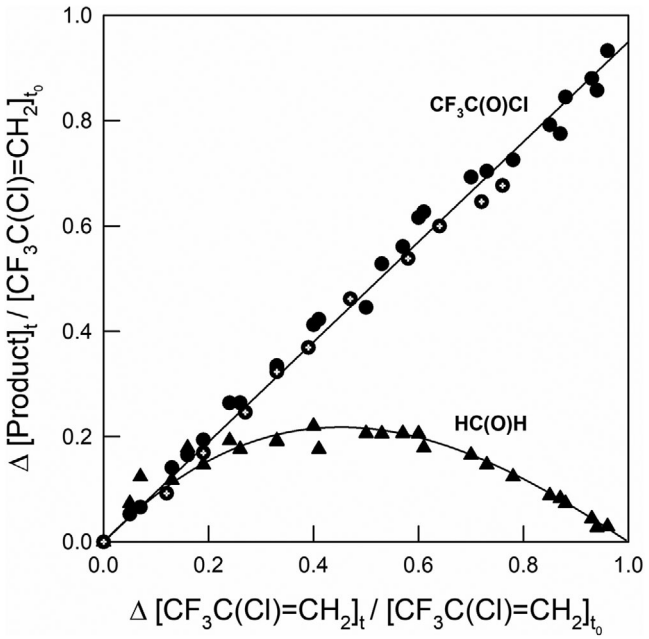

FIGURE 8 | Yields of $CF_3C(O)Cl$ (circles) and HC(O)H (triangles) against the loss of $CF_3C(Cl){=}CH_2$, normalized to initial concentration of $CF_3C(Cl){=}CH_2$ in the OH initiated oxidation of $CF_3C(Cl){=}CH_2$ in 700 Torr air of diluent. Crossed symbols were obtained using CH_3ONO as an OH source, all other data using O_3/H_2 mixtures. The fit to the HC(O)H data is a non-linear fit (see main text for details) while the line thorough the $CF_3C(O)Cl$ data is a linear least square fit.

$$OH + CF_3C(Cl){=}CH_2 \rightarrow CF_3ClC(\cdot){-}CH_2(OH) \quad (45a)$$

$$OH + CF_3C(Cl){=}CH_2 \rightarrow CF_3ClC(OH){-}CH_2(\cdot) \quad (45b)$$

The alkoxy radical generated from the addition of OH to the terminal carbon (reaction 45a) will give $CF_3C(O)Cl$ and HC(O)H though the following reactions steps:

$$CF_3ClC(\cdot){-}CH_2(OH) + O_2 \rightarrow CF_3ClCO_2(\cdot){-}CH_2(OH) \quad (46)$$

$$CF_3ClCO_2(\cdot){-}CH_2(OH) + RO_2(\cdot) \rightarrow CF_3ClCO(\cdot){-}CH_2(OH) + RO(\cdot) + O_2 \quad (47)$$

The resulting alkoxy radicals will undergo decomposition through C–C scission:

$$CF_3ClCO(\cdot){-}CH_2(OH) \rightarrow CF_3C(O)Cl + (\cdot)CH_2(OH) \quad (48)$$

$$(\cdot)CH_2(OH) + O_2 \rightarrow HC(O)H + HO_2 \quad (49)$$

The alkoxy radical generated in reaction (47) could undergo Cl-elimination too:

$$CF_3ClCO(\cdot){-}CH_2(OH) \rightarrow CF_3C(O)CH_2(OH) + Cl \quad (50)$$

However, no carbonyl features were observed in the product spectra, besides those that can be ascribed to the formation of HC(O)H and $CF_3C(O)Cl$, hence, reaction (50) would likely be of minor importance.

The alkyle radical $CF_3ClC(OH){-}CH_2(\cdot)$, generated in reaction (45b), could react with O_2 or undergo decomposition:

$$CF_3ClC(OH)CH_2(\cdot) + O_2 \rightarrow CF_3ClC(OH)CH_2O_2(\cdot) \quad (51)$$

$$CF_3ClC(OH){-}CH_2(\cdot) \rightarrow CF_3C(OH){=}CH_2 + Cl \quad (52)$$

The alkoxy radical is an alpha chlorine substituted alcohol, and by analogy to the observed behavior of products of *(E)*- and *(Z)*-$CF_3CH{=}CHCl$ [23, 24], we believe that $CF_3ClC(OH){-}CH_2(\cdot)$ will undergo decomposition via Cl elimination on a timescale too short for bimolecular reaction with O_2 to be able to compete efficiently, and yield prop-1-en-2-ol, $CF_3C(OH){=}CH_2$. No indication of formation of the enol was seen in the product spectra (enols have a characteristic OH band in the stretch region (3300–3700 cm^{-1}). The enol may also tautomerize to the acetonyl compound $CF_3C(O)CH_3$, however there was also no indication of $CF_3C(O)CH_3$ in the product spectra.

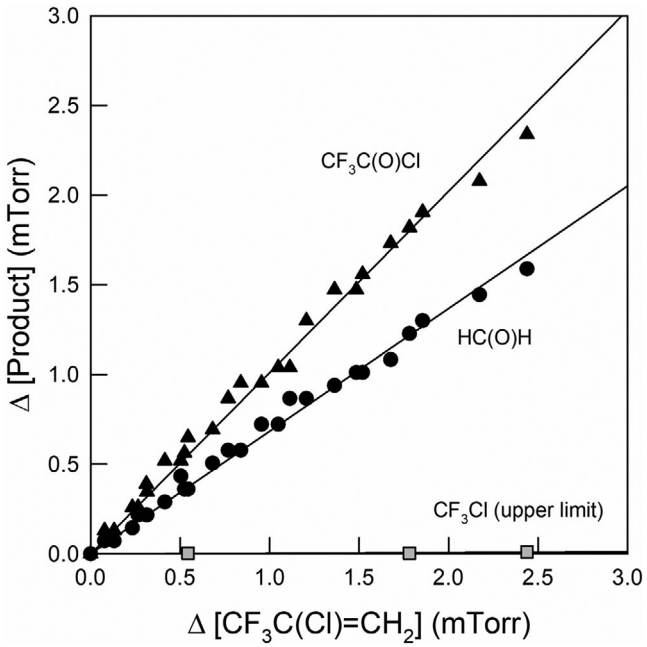

FIGURE 9 | Yields of $CF_3C(O)Cl$ (triangles) and HC(O)H (circles) following the O_3 initiated oxidation of $CF_3C(Cl)=CH_2$ in 700 Torr air of diluent. Estimated upper limits to the formation of CF_3Cl are shown with gray squares. The lines through the data are linear least square regressions.

If $CF_3ClC(OH)CH_2(\cdot)$ does not undergo Cl elimination, the peroxy radical generated in reaction (51) will undergo reaction with RO_2 to give $CF_3ClC(OH)CH_2O(\cdot)$. The main fates expected for $CF_3ClC(OH)CH_2O(\cdot)$ would be reaction with O_2 to give a carbonyl compound:

$$CF_3ClC(OH)CH_2O(\cdot) + O_2 \rightarrow CF_3ClC(OH)CHO + HO_2 \quad (53)$$

or C–C bond scission:

$$CF_3ClC(OH)CH_2O(\cdot) \rightarrow HC(O)H + CF_3ClC(OH)(\cdot) \quad (54)$$

$$CF_3ClC(OH)(\cdot) + O_2 \rightarrow CF_3C(O)Cl + HO_2 \quad (55)$$

The observed yields of $CF_3C(O)Cl$ and HC(O)H, the only two products observed, are indistinguishable from unity and account for a full carbon balance. However, since addition of OH to either side of the double bond could potentially lead to the formation of $CF_3C(O)Cl$ and HC(O)H, we cannot say conclusively if OH adds preferentially to the terminal or the central carbon in $CF_3C(Cl)=CH_2$.

3.7 | Product Study of $CF_3C(Cl)=CH_2 + O_3$

The products formed from the reaction of O_3 with $CF_3ClC=CH_2$ were investigated using starting reaction mixtures of 5.1–5.7 mTorr of $CF_3ClC=CH_2$, and 0.35–2.8 mTorr O_3 diluted in air at 700 Torr with an OH radical scavenger, *c*-C_6H_{12} 10–20 mTorr. Two sole products, $CF_3C(O)Cl$ and HC(O)H, were observed as products of the ozonolysis reaction. The formation of products versus the degradation of $CF_3C(Cl)=CH_2$ is shown in Figure 9. The lines through the data in Figure 9 are linear least squares fits giving yields of (101 ± 5)%, and (68 ± 3)%, for $CF_3C(O)Cl$ and HC(O)H, respectively. No other carbon containing products were identified in the product spectra, with the exception of CO_2. Due to persistent, but varied residual signal of CO_2 in our system, this is not a good mechanistic marker for the reaction in our system.

The addition of O_3 to $CF_3C(Cl)=CH_2$ leads to the formation of a primary ozonide (POZ). The POZ generated here undergoes unimolecular decomposition through two channels leading to formation of energy rich Criegee intermediates and a carbonyl containing species:

$$POZ \rightarrow CF_3C(O)Cl + [H_2COO]^* \quad (56a)$$

$$\rightarrow HC(O)H + [CF_3CClOO]^* \quad (56b)$$

The Criegee intermediates formed in reactions (56a) and (56b) can undergo both fragmentation and collisional stabilization. Garavagno et al. [10] observed the subsequent rearrangement of CF_3CClOO (generated in reaction 56b) into CF_3Cl as a stable end-product and reported a yield of 0.034% (upper limit 0.043%, lower limit of 0.028%). In the present experiments, IR features attributable to CF_3Cl were sought using reported cross sections for CF_3Cl in the HITRAN database (1065–1140 cm^{-1}) [25, 26]. No formation of CF_3Cl was observed, and we estimate an upper limit of 0.3% for the formation of CF_3Cl (see gray symbols in Figure 9). This upper limit is consistent with the findings of Garavagno et al. [10]. It is interesting that a yield indistinguishable from unity for $CF_3C(O)Cl$ is observed while the total carbon balance does not add to unity. We hypothesize that most of the decomposition of the POZ occurs through reaction (56a) and that the fate of $[H_2COO]^*$ is mainly fragmentation to products, including, but not exclusively HC(O)H.

4 | Implications for Atmospheric Chemistry

Halogenated olefins, including $CF_3C(Cl)=CH_2$, do not photolyze in the actinic region of the electromagnetic spectrum [27], nor are they expected to undergo wet or dry deposition to any significant extent. Although the Cl atom rate constant for $CF_3C(Cl)=CH_2$ is larger than the OH rate constant (see Table 2), the global average concentration of Cl atoms in the atmosphere is in general much lower than that of OH radicals, $[Cl]_{global\ average} = 1 \times 10^3$ molecule cm^{-3} [28] versus $[OH]_{global\ average} = 1 \times 10^6$ molecule cm^{-3} [29]. With regard to the reaction with ozone, using the rate constant k_8 determined herein and assuming a moderately polluted atmosphere, with an ozone concentration of 50 ppb, the fraction of $CF_3C(Cl)=CH_2$ which react with ozone in the atmosphere can be estimated to be on the order of 0.1%. The contribution of the reaction of ozone with $CF_3C(Cl)=CH_2$ to the atmospheric burden of CF_3Cl will be small. We predict that the atmospheric lifetime of $CF_3C(Cl)=CH_2$ is almost exclusively governed by the reaction with OH radicals.

Using the OH radical and Cl atom rate constants determined herein, and the global average concentrations listed above, we estimate the atmospheric lifetime of $CF_3C(Cl)=CH_2$ to be approximately 3.3 days. An atmospheric lifetime this short will impart a strong spatial inhomogeneity in the atmospheric distribution

TABLE 2 | Summary of rate constants determined in the present work for $CF_3C(Cl)=CH_2$ at 295± 2 K and 700 Torr total pressure, as well as literature values for the rate constants for two similar isomers.

Compound	k_{Cl} (cm^3 $molecule^{-1}$ s^{-1})	k_{OH} (cm^3 $molecule^{-1}$ s^{-1})	k_{O3} (cm^3 $molecule^{-1}$ s^{-1})
$CF_3C(Cl)=CH_2$	$(8.3 \pm 1.1) \times 10^{-11}$ (present work)	$(3.4 \pm 0.8) \times 10^{-12}$ (present work) 1.31×10^{-12} (Garavagno et al. [10])	$(2.50 \pm 0.10) \times 10^{-21}$ (present work) $(2.54 \pm 0.36) \times 10^{-21}$ (McGillen et al. [9])
(*Z*)-$CF_3CH=CHCl$	$(6.26 \pm 0.84) \times 10^{-11}$ [14]	3.53×10^{-13} [19]	$(1.53 \pm 0.12) \times 10^{-21}$ [14]
(*E*)-$CF_3CH=CHCl$	$(5.22 \pm 0.72) \times 10^{-11}$ [15]	9.24×10^{-13} [19]	$(1.46 \pm 0.12) \times 10^{-21}$ [15]

of $CF_3C(Cl)=CH_2$ emitted to the atmosphere. Furthermore, the vertical distribution of $CF_3C(Cl)=CH_2$ will be limited and any contribution to the Cl-atom catalyzed depletion of ozone in the stratosphere will be negligible. The atmospheric lifetime and ODP of (*E*)-$CF_3CH=CHCl$ has been estimated at ~40 days and ~10^{-4}, respectively [30]. With a lifetime of 3.3 days, the ODP of $CF_3C(Cl)=CH_2$ will be lower than that for (*E*)-$CF_3CH=CHCl$.

The GWP of $CF_3C(Cl)=CH_2$ can be calculated according to Equation (III),

$$GWP(t) = \frac{\int_0^{t'} RE_{CF_3C(Cl)=CH_2} \exp\left(-t/\tau_{CF_3C(Cl)=CH_2}\right) dt}{\int_0^{t'} RE_{CO_2} R(t)\, dt} \quad \text{(III)}$$

where RE_{CO_2} and $RE_{CF_3C(Cl)=CH_2}$ are the radiative efficiencies of CO_2 and $CF_3C(Cl)=CH_2$, respectively, $\tau_{CF_3C(Cl)=CH_2}$ is the atmospheric lifetime of $CF_3C(Cl)=CH_2$, t is the time horizon and $R(t)$ is the response function that describes the decay of an instantaneous pulse of CO_2. The denominator in Equation (III) is the absolute global warming potential (AGWP) for CO_2. With concentrations of CO_2 continuing to increase the AGWP will steadily decrease. Here, we choose to use the AGWPs determined in Hodnebrog et al. [31] as 2.29×10^{-14}, 8.06×10^{-14}, 2.694×10^{-13} W m^{-2} kg^{-1} for 20, 100, and 500-year time horizons, respectively. With the IR spectrum for $CF_3C(Cl)=CH_2$ shown in Figure 4 and the updated 10 cm^{-1} narrow band model by Pinnock et al. [32, 33], we calculate an estimated radiative efficiency for $CF_3C(Cl)=CH_2$ as 0.179 W m^{-2} ppb^{-1}. Because $CF_3C(Cl)=CH_2$ has a short lifetime and therefore will not be homogenously distributed in the atmosphere, this estimated RE value needs to be adjusted. We use the correction factor by Hodnebrog et al. [31] (Equation IV) that adjusts for non-uniform horizontal and vertical mixing in the atmosphere:

$$f(\tau) = \frac{a\,\tau^b}{1 + c\,\tau^d} \quad \text{(IV)}$$

where the constants a, b, c, and d, are given as 2.962, 0.9312, 2.994, and 0.9302, respectively. Using Equation (IV) to correct the calculated RE for non-uniform mixing, we determine an effective radiative efficiency for HCFO-1233xf of 0.007 W m^{-2} ppb^{-1}. The GWPs for $CF_3C(Cl)=CH_2$, accounting for non-uniform horizontal and vertical mixing, can then be determined from expression (III) giving values of 0.109, 0.031 and 0.009 for the 20, 100, and 500-year horizons, respectively.

The environmental fate of HC(O)Cl is incorporation into rain, cloud, and fog water, followed by hydrolysis to give formic acid and wet deposition, within probably 5–15 days [34]. Formic acid is a ubiquitous component of the environment and is of no concern. The other oxidation product, $CF_3C(O)Cl$, is expected to undergo photolysis in competition with uptake into water droplets followed by hydrolysis. An estimated 60%, on average, of $CF_3C(O)Cl$ in the troposphere is converted into $CF_3C(O)OH$ (TFA) [35]. There are sources of TFA to the environment, including the degradation of certain CFC-replacement compounds, pesticides and pharmaceuticals. TFA is persistent and ubiquitous in the environment, natural sources have been suggested, and concentrations are increasing globally. There is ongoing debate about the sources, fate, and toxicity of TFA [36]. No atmospheric detections of $CF_3C(Cl)=CH_2$ have been reported in the literature to date. However, at the anticipated levels in the environment, the impacts of $CF_3C(Cl)=CH_2$ on stratospheric ozone depletion, and on the radiative forcing of climate change will be negligible.

Acknowledgments

TM acknowledges support from the National Science Foundation (CHE -2506192).

Conflicts of Interest

The authors declare no conflicts of interest.

Data Availability Statement

The data that support the findings of this study are available from the corresponding author upon reasonable request.

References

1. M. J. Molina and F. S. Rowland, "Stratospheric Sink for Chlorofluoromethanes: Chlorine Atom-Catalysed Destruction of Ozone," *Nature* 249 (1974): 810–812, https://doi.org/10.1038/249810a0.

2. J. C. Farman, B. G. Gardiner, and J. D. Shanklin, "Large Losses of Total Ozone in Antarctica Reveal Seasonal ClOx/NOx Interaction," *Nature* 315 (1985): 207–210, https://doi.org/10.1038/315207a0.

3. S. Solomon, R. R. Garcia, F. S. Rowland, and D. J. Wuebbles, "On the Depletion of Antarctic Ozone," *Nature* 321 (1986): 755–758, https://doi.org/10.1038/s41586-025-08640-9.

4. L. Hu, S. A. Montzka, and S. J. Lehmann, "Considerable Contribution of the Montreal Protocol to Declining Greenhouse Gas Emissions From the United States," *Geophysical Research Letters* 44 (2017): 8075–8083, https://doi.org/10.1002/2017GL074388.

5. S. Mukhopadhyay, B. A. Light, K. M. Fleming, S. D. Phillips, and R. K. Dubey, "Gas Phase Synthesis of 2,3,3,3-Tetrafluoro-1propene From 2-Chloro-3,3,3-Trifluoro-1-Propene ES 23,818,85T 3," (2009).

6. D. C. Merkel and H. S. Tung, "Method for Producing 2-Chloro-3,3,3,-Trifluoropropene (HCFC-1233xf) US 8,119,845 B2," (2012).

7. G. Yang, L. Xu, and H. Yang, "Method for Preparing 2,3,3,3-Tetrafluoropropene US 9,115,042 B2," (2015).

8. R. Hu, C. Zhang, F. Qing, and H. Quan, "Synthesis of 2,3,3,3-Tetrafluoropropene via Vapor-Phase Catalytic Fluorination in the Presence of Cr-Based Catalyst," *Journal of Fluorine Chemistry* 185 (2016): 187–190, https://doi.org/10.1016/j.jfluchem.2016.03.015.

9. M. R. McGillen, Z. T. P. Fried, and M. A. H. Khan, "Ozonolysis Can Produce Long-Lived Greenhouse Gases From Commercial Refrigerants," *Proceedings of the National Academy of Sciences* 120 (2023): e2312714120, https://doi.org/10.1073/pnas.2312714120.

10. M. D. L. A. Garavagno, A. Wenger, and R. E. T. Holland, "Atmospheric Oxidation of Hydrofluoroolefins and Hydrochlorofluoroolefins by Ozone Produces HFC-23, PFC-14, and CFC-13," *Environmental Science & Technology* 59 (2025): 26031–26040, https://doi.org/10.1021/acs.est.5c11383.

11. World Meteorological Organization Scientific Assessment of Ozone Depletion: 2022; WMO: Geneva, 2022.

12. T. J. Wallington, J. M. Andino, I. M. Lorkovic, E. W. Kaiser, and G. Marston, "Pressure Dependence of the Reaction of Chlorine Atoms With Ethene and Acetylene in Air at 295 K," *Journal of Physical Chemistry* 94, no. 9 (1990): 3644–3648, https://doi.org/10.1021/j100372a052.

13. S. P. Sander, J. P. D. Abbatt, and J. R. Barker, "Chemical Kinetics and Photochemical Data for Use in Atmospheric Studies: Evaluation No. 17, JPL Publication 10-6, Jet Propulsion Laboratory," (2011), Pasadena.

14. L. L. Andersen, F. F. Østerstrøm, M. P. Sulbaek Andersen, O. J. Nielsen, and T. J. Wallington, "Atmospheric Chemistry of Cis-CF3CH═CHCl (HCFO-1233zd(Z)): Kinetics of the Gas-Phase Reactions With Cl Atoms, OH radicals, and O_3," *Chemical Physics Letters* 639 (2015): 289–293, https://doi.org/10.1016/j.cplett.2015.09.008.

15. M. P. S. Andersen, E. J. K. Nilsson, O. J. Nielsen, M. S. Johnson, M. D. Hurley, and T. J. Wallington, "Atmospheric Chemistry of Trans-CF3CH CHCl: Kinetics of the Gas-Phase Reactions With Cl Atoms, OH Radicals, and O3," *Journal of Photochemistry and Photobiology A: Chemistry*, 199, 1 (2008): 92–97, https://doi.org/10.1016/j.jphotochem.2008.05.013.

16. M. Sørensen, E. W. Kaiser, M. D. Hurley, T. J. Wallington, and O. J. Nielsen, "Kinetics of the Reaction of OH Radicals With Acetylene in 25–8000 Torr of Air at 296 K," *International Journal of Chemical Kinetics* 35 (2003): 191, https://doi.org/10.1002/kin.10119.

17. J. G. Calvert, R. Atkinson, and J. A. Kerr, *The Mechanisms of Atmospheric Oxidation of the Alkenes* (Oxford University Press, 2000).

18. L. Michelat, A. Mellouki, A. Ravishankara, H. El Othmani, V. C. Papadimitriou, and V. Daële, "Temperature-Dependent Structure–Activity Relationship of OH + Haloalkene Rate Coefficients under Atmospheric Conditions and Supporting Measurements," *ACS Earth and Space Chemistry* 6, no. 12 (2022): 3101–3114, https://doi.org/10.1021/acsearthspacechem.2c00296.

19. IUPAC Task Group on Atmospheric Chemical Kinetic Data Evaluation, This data sheet last evaluated: June 2023; last change in preferred values: January 2023. Accessed July 9 2025, https://iupac.aeris-data.fr/.

20. J. G. Calvert, R. G. Derwent, J. J. Orlando, G. S. Tyndall, and T. J. Wallington, *Mechanisms of the Atmospheric Oxidation of the Alkanes* (Oxford University Press, 2008).

21. J. G. Calvert, A. Mellouki, J. J. Orlando, M. J. Pilling, and T. J. Wallington, *Mechanisms of Atmospheric Oxidation of the Oxygenates* (Oxford University Press, 2011).

22. R. J. Meagher, M. E. McIntosh, M. D. Hurley, and T. J. Wallington, "A Kinetic Study of the Reaction of Chlorine and Fluorine Atoms With HC(O)F at 295±2 K," *International Journal of Chemical Kinetics* 29 (1997): 619–625, https://doi.org/10.1002/(SICI)1097-4601(1997)29:8⟨619::AID-KIN7⟩3.0.CO;2-X.

23. M. P. Sulbaek Andersen, O. J. Nielsen, M. D. Hurley, and T. J. Wallington, "Atmospheric Chemistry of *t*-CF_3CH═CHCl: Products and Mechanisms of the Gas-Phase Reactions With Chlorine Atoms and Hydroxyl Radicals," *Physical Chemistry Chemical Physics* 14 (2012): 1735–1748, https://doi.org/10.1039/C1CP22925G.

24. M. P. Sulbaek Andersen, T. I. Soelling, and L. L. Andersen, "Atmospheric Chemistry of (*Z*)-CF_3CH═CHCl: Products and Mechanisms of the Cl Atom, OH Radical and O_3 Reactions, and Role of (E)–(Z) isomerization," *Physical Chemistry Chemical Physics* 20 (2018): 27949–27958, https://doi.org/10.1039/C8CP04903C.

25. I. E. Gordon, L. S. Rothman, and R. J. Hargreaves, "The HITRAN2024 molecular spectroscopic database," *Journal of Quantitative Spectroscopy and Radiative Transfer* 353 (2026): 109807, https://doi.org/10.1016/j.jqsrt.2026.109807.

26. A. H. McDaniel, C. A. Cantrell, J. A. Davidson, R. E. Shetter, and J. G. Calvert, "The Temperature Dependent, Infrared Absorption Cross Sections for the Chlorofluorocarbons: CFC-11, CFC-12, CFC-13, CFC-14, CFC-22, CFC-113, CFC-114, and CFC-115," *Journal of Atmospheric Chemistry* 12 (1991): 211–227, https://doi.org/10.1007/BF00048074.

27. R. J. Cicerone and R. Zellner, "The Atmospheric Chemistry of Hydrogen Cyanide (HCN)," *Journal of Geophysical Research, [Atmospheres]* 88 (1983): 10689–10696, https://doi.org/10.1029/JC088iC15p10689.

28. X. Wang, D. J. Jacob, and S. D. Eastham, "The Role of Chlorine in Global Tropospheric Chemistry," *Atmospheric Chemistry and Physics* 19 (2019): 3981–4003, https://doi.org/10.5194/acp-19-3981-2019.

29. R. G. Prinn, J. Huang, and R. F. Weiss, *Science* 292 (2001): 1882–1888, https://doi.org/10.1126/science.1058673.

30. M. P. Sulbaek Andersen, J. A. Schmidt, A. Volkova, and D. J. Wuebbles, "A Three-Dimensional Model of the Atmospheric Chemistry of E and Z-CF_3CH═CHCl (HCFO-1233(zd) (E/Z))," *Atmospheric Environment* 179 (2018): 250–259, https://doi.org/10.1016/j.atmosenv.2018.02.018.

31. Ø. Hodnebrog, B. Aamaas, and J. S. Fuglestvedt, "Updated Global Warming Potentials and Radiative Efficiencies of Halocarbons and Other Weak Atmospheric Absorbers," *Reviews of Geophysics* 58 (2020): e2019RG000691.

32. S. Pinnock, M. D. Hurley, K. P. Shine, T. J. Wallington, and T. J. Smyth, "Radiative Forcing of Climate by Hydrochlorofluorocarbons and Hydrofluorocarbons," *Journal of Geophysical Research: Atmospheres* 100 (1995): 23227–23238, https://doi.org/10.1029/95JD02323.

33. K. P. Shine and G. Myhre, "The Spectral Nature of Stratospheric Temperature Adjustment and Its Application to Halocarbon Radiative Forcing," *JAMES* 12 (2020): e2019MS001951, https://doi.org/10.1029/2019MS001951.

34. T. J. Wallington, W. F. Schneider, and D. R. Worsnop, "The Environmental Impact of CFC Replacements HFCs and HCFCs," *Environmental Science & Technology* 28 (1994): 320A–326A, https://doi.org/10.1021/es00056a714.

35. G. D. Hayman, M. E. Jenkin, T. P. Murrells, and C. E. Johnson, "Tropospheric Degradation Chemistry of HCFC-123 (CF_3CHCl_2): A Proposed Replacement Chlorofluorocarbon," *Atmospheric Environment* 28 (1994): 421–437, https://doi.org/10.1016/1352-2310(94)90121-X.

36. M. L. Hanson, S. Madronich, K. Solomon, M. P. Sulbaek Andersen, and T. J. Wallington, "Trifluoroacetic Acid in the Environment: Consensus, Gaps, and Next Steps," *Environmental Toxicology and Chemistry* 43 (2024): 2091–2093, https://doi.org/10.1002/etc.5963.